Random ocean swell-rays: a stochastic framework

Valentin Resseguier, Erwan Hascoët, Bertrand Chapron

Random ocean swell-rays: a stochastic framework

Valentin Resseguier[1], Erwan Hascoët[2], Bertrand Chapron[3]

[1] Lab, SCALIAN DS,
valentin.resseguier@scalian.com,
home page: https://sites.google.com/view/valentinresseguier
[2] OceanDataLab, France
[3] Laboratoire d'Océanographie Physique et Spatiale (LOPS), Ifremer, France

1 Introduction

Originating from distant storms, swell systems radiate across all ocean basins (Snodgrass et al, 1966; Collard et al, 2009; Ardhuin et al, 2009). Far from their sources, emerging surface waves have low steepness characteristics, with very slow amplitude variations. Swell propagation then closely follows principles of geometrical optics, i.e. the eikonal approximation to the wave equation, with a constant wave period along geodesics, when following a wave packet at its group velocity. The phase averaged evolution of quasi-linear wave fields is then dominated by interactions with underlying current and/or topography changes (Phillips, 1977). Comparable to the propagation of light in a slowly varying medium, over many wavelengths, cumulative effects can lead to refraction, i.e. change of the direction of propagation of a given wave packet, so that it departs from its initial ray-propagation direction. This opens the possibility of using surface swell systems as probes to estimate turbulence along their propagating path.

For a single progressive swell wave train, a description of the form

$$h(\boldsymbol{x},t) = a(\boldsymbol{x},t)e^{i\phi(\boldsymbol{x},t)}, \tag{1.1}$$

is locally possible for most wave properties, i.e. the surface elevation, slope, orbital velocities. If the wave-ray propagation is to be followed, or predicted, the phase, $\phi(\boldsymbol{x},t)$, must vary smoothly along the wave's path. Mathematically, $\phi(\boldsymbol{x},t)$ is required to be differentiable, to define the relative frequency

$$\omega = -\partial_t\phi(\boldsymbol{x},t), \tag{1.2}$$

and the wave number vector

$$\boldsymbol{k} = \boldsymbol{\nabla}\phi(\boldsymbol{x},t). \tag{1.3}$$

These partial derivatives of $\phi(\boldsymbol{x},t)$ being independent of the differentiation order, the kinematical conservation equation for the density of waves writes

$$-\boldsymbol{\nabla}\omega = \partial_t\boldsymbol{k}, \tag{1.4}$$

with the irrotational condition

$$\boldsymbol{\nabla} \times \boldsymbol{k} = 0, \tag{1.5}$$

to serve as an initial condition for use with Kelvin's circulation theorem. The rate of change of the wave-number is balanced by the convergence of the frequency, the number of wave crests passing a fixed point.

Let us now consider an ocean moving with velocity $\boldsymbol{v}$, slowly varying with respect to time and space. The frequency of wave crests passing a fixed point, i.e. the apparent frequency, becomes

$$\omega = \omega_0 + \boldsymbol{v} \cdot \boldsymbol{k}, \tag{1.6}$$

with $\omega_0 = f(\boldsymbol{k}, H)$, H the depth, the intrinsic frequency, whose functional dependence on $\boldsymbol{k}$ is known. For gravity waves, this dispersion relationship is

$$\omega_0 = \sqrt{g\|\boldsymbol{k}\| \tanh \|\boldsymbol{k}\| H}, \tag{1.7}$$

and thus

$$\partial_t \boldsymbol{k} + \partial_k \omega_0 \boldsymbol{\nabla} \boldsymbol{k} + \partial_H \omega_0 \boldsymbol{\nabla} H + \boldsymbol{l} \cdot \boldsymbol{v} \boldsymbol{\nabla} \|\boldsymbol{k}\| + \|\boldsymbol{k}\| \boldsymbol{\nabla} (\boldsymbol{l} \cdot \boldsymbol{v}) = 0, \tag{1.8}$$

with $\boldsymbol{l}$ is a unit vector in the direction of $\boldsymbol{k}$ and $k = \|\boldsymbol{k}\|$. Consequently, for a steady wave train, the variation of the wave-number magnitude along the propagation s is

$$\partial_s \|\boldsymbol{k}\| = -(c_g + \boldsymbol{l} \cdot \boldsymbol{v})^{-1} [\partial_H \omega_0 \partial_s H + \|\boldsymbol{k}\| \partial_s (\boldsymbol{l} \cdot \boldsymbol{v})], \tag{1.9}$$

with $c_g = \partial_k \omega_0$, the local group velocity. Using the irrotational condition, the evolution of the ray direction, $\theta(s)$, follows

$$\partial_s \theta = -(c_g + \boldsymbol{l} \cdot \boldsymbol{v})^{-1} [\frac{1}{\|\boldsymbol{k}\|} \partial_H \omega_0 \partial_\nu H + \partial_\nu (\boldsymbol{l} \cdot \boldsymbol{v})], \tag{1.10}$$

where ν is a unit vector normal to the direction of the ray. Accordingly, wave trajectories will bend with depth variations. For deep water, the dispersion relationship reduces to $\omega_0 = \sqrt{g\|\boldsymbol{k}\|}$, and $\theta(s)$ solely depends upon the ratio between the cross-ray current gradient and the local group velocity. More generally, this result extends to the ray curvature, being to first order controlled by ζ / c_g, the ratio between $\zeta = \boldsymbol{\nabla} \times \boldsymbol{v}$, the vertical component of the current vorticity, and $c_g = \partial_k \omega_0 = \omega / 2\|\boldsymbol{k}\|$, the group velocity. Accordingly, the rays will bend in the direction of decreasing (increasing) current speed. Moreover, a potential velocity field will give little refraction. Yet, a potential velocity field will control the variation of the wave-number magnitude, and thus the group velocity and bending, along the propagation.

To specify the local linear wave propagation, a precise knowledge of the surface currents, local gradients and/or vorticity, thus appears essential. In a realistic numerical setting, Ardhuin et al (2017) clearly demonstrated that wave energy

variations would largely be dominated by the effects of ocean currents at scales of about 10 to 100 km. From altimeter ocean surface wave energy measurements, Quilfen and Chapron (2019) also showed that mesoscale and sub-mesoscale upper ocean circulation can drive a significant part of the wave variability in the coupled ocean-atmosphere system. Unfortunately, these small-scale currents are not observed and certainly not resolved in operational models. Today, a precise spatio-temporal information is thus largely missing. To overcome these observation difficulties, but to best take into account unresolved small-scale currents, a stochastic framework can be adopted. Such a stochastic model shall then provide means to perform fast simulations and test ensembles of wave-propagation predictions, to best evaluate impacts of underlying near-surface small-scale currents on the evolution of ocean surface swell systems.

2 Random Swell-Rays

To first order in wave steepness, the group velocity $\boldsymbol{v}_g$ is modified by the local velocity of the currents $\boldsymbol{v}$,

$$\frac{d\boldsymbol{x}}{dt} = \boldsymbol{v}_g = \boldsymbol{\nabla}_{\boldsymbol{k}}\omega = \underbrace{\boldsymbol{\nabla}_{\boldsymbol{k}}\omega_0(\boldsymbol{k})}_{\substack{\text{Group velocity}\\ \text{without currents}\\ \text{but changing wave vector}}} + \boldsymbol{v}, \tag{2.1}$$

where $\boldsymbol{x}$ is the centroid of a wave group. The ray direction can thus differ from the direction of the wave vector, except in the case of parallel wave and current directions. Unlike depth refraction, the crest alignment does not indicate the wave propagation direction. The coupled wave vector evolution writes

$$\frac{d\boldsymbol{k}}{dt} = -\boldsymbol{\nabla}\boldsymbol{v}^T\boldsymbol{k}. \tag{2.2}$$

Along the propagation ray, velocity gradients induce linear variations. Decelerating currents will shorten waves, and thus reduce the group velocity. The validity of this coupled ray approximation largely depends on the condition $\|\boldsymbol{k}\|\xi \gg 1$, where ξ is a length scale on which the current field is varying, physically corresponding to the typical eddy size. This condition is well satisfied for wave numbers of interest, of order $\|\boldsymbol{k}\| \sim 2\pi/250$ rad.m^{-1}, and typical eddy size $\xi \sim 5$ km or larger. Scattering of the waves by currents can further be assumed to be weak, with $\|\boldsymbol{v}\|$ of order 0.5 m/s, much smaller than $\|\boldsymbol{v}_g\|$ of order 10 m/s. Subsequently, each ray will be appreciably deflected, with scattering angle of order $\sim \|\boldsymbol{v}\|/\|\boldsymbol{v}_g\|$ after traveling a typical correlation length $\sim \xi$ along the mean wave vector direction.

To complete the wave field description, the wave action $A(\boldsymbol{x}, t)$ is considered to be an adiabatic invariant. Wave action is crucial to anticipate wave transformations by currents (White and Fornberg, 1998). This action is the integral of the action spectrum $N(\boldsymbol{x}, \boldsymbol{k}, t)$ over all the wave-vectors $\boldsymbol{k}$:

$$A(\boldsymbol{x}, t) = \int d\boldsymbol{k}\ N(\boldsymbol{x}, \boldsymbol{k}, t). \tag{2.3}$$

The wave action spectrum N is the action by unit of surface (unit of $\boldsymbol{x}$) and by unit of wave-vector surface (unit of $\boldsymbol{k}$). For linear waves, the wave action spectrum is simply related to the wave energy spectrum E:

$$E(\boldsymbol{x},\boldsymbol{k},t) = N(\boldsymbol{x},\boldsymbol{k},t)\ \omega_0(\boldsymbol{k}). \tag{2.4}$$

By the Liouville theorem, the $(\boldsymbol{x},\boldsymbol{k})$ space does not contract nor dilate along time[4]. Since the dissipation is neglected, the wave action spectrum N is thus conserved (Lavrenov, 2013), i.e.

$$N\left(\boldsymbol{x}(t_i),\boldsymbol{k}(t_i),t_i\right) = N\left(\boldsymbol{x}(t_f),\boldsymbol{k}(t_f),t_f\right), \tag{2.5}$$

along the following $(\boldsymbol{x},\boldsymbol{k})$ variable change between initial time t_i and the final time t_f:

$$\begin{pmatrix}\boldsymbol{x}(t_i)\\ \boldsymbol{k}(t_i)\end{pmatrix} \mapsto \begin{pmatrix}\boldsymbol{x}(t_f)\\ \boldsymbol{k}(t_f)\end{pmatrix}. \tag{2.6}$$

Subsequently, each Fourier mode of a swell wave train can be modified, independently of the others. In absence of source terms, the action spectrum conservation (2.5) then writes:

$$\frac{dN}{dt} = \partial_t N + \boldsymbol{v}_g \cdot \boldsymbol{\nabla}_{\boldsymbol{x}} N + \left(-\boldsymbol{\nabla}_{\boldsymbol{x}}\boldsymbol{v}^T\boldsymbol{k}\right)\cdot\boldsymbol{\nabla}_{\boldsymbol{k}} N = 0. \tag{2.7}$$

3 The time-decorrelation assumption

Now, the Eulerian current $\boldsymbol{v}$ is decomposed into a large-scale component $\overline{\boldsymbol{v}}$ and a small-scale unresolved component $\boldsymbol{v}'$:

$$\boldsymbol{v} = \overline{\boldsymbol{v}} + \boldsymbol{v}'. \tag{3.1}$$

In a stochastic framework, we can work with the Stratonovich notations (Oksendal, 1998; Kunita, 1997). Under Stratonovich calculus rules, expressions become similar to deterministic ones. The Stratonovich dispersion relation is analogous to the deterministic one (1.6). The method of characteristics is also valid, (2.1), (2.2), and (2.5), with $\boldsymbol{v}'$ defined by $\boldsymbol{\sigma}\circ \mathrm{d}B_t/dt$, where $\mathrm{d}B_t/dt$ is a spatio-temporal white noise and $\boldsymbol{\sigma}\circ$ denotes a spatial filter which encodes spatial correlations and horizontal incompressibility ($\boldsymbol{\nabla}\cdot\boldsymbol{\sigma} = 0$). For a spatially stationary and isotropic small-scale velocity, the wave characteristic dynamics equations (2.1), (2.2) and (2.5) would then also remain the same with Ito notations (i.e. we can replace $\boldsymbol{\sigma}\circ\mathrm{d}B_t$ by $\boldsymbol{\sigma}\mathrm{d}B_t$ to derive the evolution). With Ito notations, the action spectrum conservation (2.7) writes

$$\partial_t N + \boldsymbol{v}_g \cdot \boldsymbol{\nabla}_{\boldsymbol{x}} N + \left(-\boldsymbol{\nabla}_{\boldsymbol{x}}\boldsymbol{v}^T\boldsymbol{k}\right)\cdot\boldsymbol{\nabla}_{\boldsymbol{k}} N = \begin{bmatrix}\boldsymbol{\nabla}_{\boldsymbol{x}}\\ \boldsymbol{\nabla}_{\boldsymbol{k}}\end{bmatrix}\cdot\left(\boldsymbol{D}\begin{bmatrix}\boldsymbol{\nabla}_{\boldsymbol{x}}\\ \boldsymbol{\nabla}_{\boldsymbol{k}}\end{bmatrix} N\right), \tag{3.2}$$

[4] $\begin{bmatrix}\boldsymbol{\nabla}_{\boldsymbol{x}}\\ \boldsymbol{\nabla}_{\boldsymbol{k}}\end{bmatrix}\cdot\left(\frac{d}{dt}\begin{bmatrix}\boldsymbol{x}\\ \boldsymbol{k}\end{bmatrix}\right) = \begin{bmatrix}\boldsymbol{\nabla}_{\boldsymbol{x}}\\ \boldsymbol{\nabla}_{\boldsymbol{k}}\end{bmatrix}\cdot\left(\begin{bmatrix}\boldsymbol{v}\\ -\boldsymbol{\nabla}_{\boldsymbol{x}}\boldsymbol{v}^T\boldsymbol{k}\end{bmatrix}\right) = \boldsymbol{\nabla}_x\cdot\boldsymbol{v} - \boldsymbol{\nabla}_x\cdot\boldsymbol{v} = 0.$

where $\boldsymbol{v}_g$ and $\boldsymbol{v}$ include the random small-scale component $\boldsymbol{v}' = \boldsymbol{\sigma} \mathrm{d}B_t/dt$, and

$$\boldsymbol{D} = \frac{1}{2dt}\mathbb{E}\left\{ \begin{bmatrix} \boldsymbol{\sigma}\mathrm{d}B_t \\ -\boldsymbol{\nabla}_{\boldsymbol{x}}(\boldsymbol{\sigma}\mathrm{d}B_t)^T\boldsymbol{k} \end{bmatrix} \begin{bmatrix} \boldsymbol{\sigma}\mathrm{d}B_t \\ -\boldsymbol{\nabla}_{\boldsymbol{x}}(\boldsymbol{\sigma}\mathrm{d}B_t)^T\boldsymbol{k} \end{bmatrix}^T \right\}. \tag{3.3}$$

Compared to (2.7), a RHS diffusive term appears, likely acting to increase the initial directional spread of the incident very directional swell components.

Voronovich (1991) and White and Fornberg (1998) discussed the joint random evolution changes of the coupled $(\boldsymbol{x}, \boldsymbol{k})$, i.e. the location and the wave vector of waves, subject to a random current $\boldsymbol{v}$. Considering the wave train to undergo slow changes over the typical time to travel through the typical correlation length of the underlying current, the joint time evolution of $(\boldsymbol{x}, \boldsymbol{k})$ can be approximated to be driven by a diffusion Markov process.

3.1 The ray Lagrangian correlation time

To apply (3.2), the covariance of the small-scale unresolved component $\boldsymbol{v}'$ – in the wave group frame – is thus to be assessed:

$$\gamma_{v'}^{X_r}(t) = \mathbb{E}\left(\boldsymbol{v}'(t', \boldsymbol{X}_r(t')) \cdot \boldsymbol{v}'(t'+t, \boldsymbol{X}_r(t'+t))\right) = \gamma_{v'}(t, \boldsymbol{X}_r(t'+t) - \boldsymbol{X}_r(t')), \tag{3.4}$$

where $\gamma_{v'}$ is the (Eulerian) spatio-temporal covariance of $\boldsymbol{v}'$, assuming statistical homogeneity, and stationarity for $\boldsymbol{v}'$. Assume a typical isotropic form for this covariance:

$$\gamma_{v'}(t, \boldsymbol{x}) = \gamma\left(\frac{|t|}{\tau_{v'}} + \frac{\|\boldsymbol{x}\|}{l_{v'}}\right), \tag{3.5}$$

then,

$$\gamma_{v'}^{X_r}(t) = \gamma\left(\frac{|t|}{\tau_{v'}} + \frac{\|\boldsymbol{X}_r(t'+t) - \boldsymbol{X}_r(t')\|}{l_{v'}}\right) = \gamma\left(\left(\frac{1}{\tau_{v'}} + \frac{\|\boldsymbol{v}_g\|}{l_{v'}}\right)|t| + O(t^2)\right), \tag{3.6}$$

for small time increment t. Therefore, $\left(\frac{1}{\tau_{v'}} + \frac{\|\boldsymbol{v}_g\|}{l_{v'}}\right)^{-1}$ is the correlation time of $\boldsymbol{v}'(t, \boldsymbol{X}_r(t))$. The same derivation is valid for $\boldsymbol{\nabla}(\boldsymbol{v}')^T(t, \boldsymbol{X}_r(t))$. Over deep ocean, the swell wave group velocity is $\|\boldsymbol{v}_g^0\| = \|\boldsymbol{\nabla}_{\boldsymbol{k}}\omega_0\| = \frac{1}{2}\sqrt{\frac{g}{\|\boldsymbol{k}\|}}$, and the along-ray correlation time of the small-scale velocity can be approximated by $l_{v'}/\|\boldsymbol{v}_g^0\|$. The ratio ϵ between this along-ray correlation time and the characteristic time of the wave group properties evolution, will then control the time decorrelation assumption of $\boldsymbol{v}'$:

$$\epsilon = \frac{l_{v'}}{\|\boldsymbol{v}_g^0\|}\|\boldsymbol{\nabla}\boldsymbol{v}^T\|. \tag{3.7}$$

Note the Eulerian small-scale velocity $\boldsymbol{v}'$ is not necessarily time uncorrelated. Yet, for small enough ϵ, the Lagrangian small-scale velocity along the ray can be considered time uncorrelated. From the expression of ϵ, such a condition depends upon:

- $\|\boldsymbol{v}_g^0\|$, increasing with the square root of the wave-group wave number. Hence, ϵ decreases with the square root of the wave-group wave-length.
- $l_{v'}$, defined by the separation between large scales $\overline{\boldsymbol{v}}$ and small scales $\boldsymbol{v}'$, e.g. the spatial filtering cutoff of the large-scale velocity $\overline{\boldsymbol{v}}$.
- $\|\boldsymbol{\nabla}\boldsymbol{v}^T\|$ – which is different from $\|\boldsymbol{\nabla}(\boldsymbol{v}')^T\|$ –, related to the overall kinetic energy (KE) and its high-wavenumber spectral slope.

3.2 Ray absolute diffusivity

The absolute diffusivity (or Kubo-type formula) usually corresponds, in the so-called diffusive regime, to the variance per unit of time of a fluid particle Lagrangian path $\frac{d\boldsymbol{X}}{dt} = \boldsymbol{v}$. It is approximately equal to the velocity variance times its correlation time. The Eulerian velocity covariance (3.5) will thus induce an absolute diffusivity

$$a = \int_0^\infty dt\ \gamma_{v'}(t, \boldsymbol{X}(t'+t) - \boldsymbol{X}(t')) \approx \gamma(0)\ \tau_{v'}. \tag{3.8}$$

Here, a wave group is followed along its propagation, and a ray absolute diffusivity slightly differs from the usual absolute diffusivity to become

$$a^{X_r} = \int_0^\infty dt\ \gamma_{v'}^{X_r}(t) \approx \left(\frac{1}{\tau_{v'}} + \frac{\|\boldsymbol{v}_g\|}{l_{v'}}\right)^{-1} \gamma(0) \approx \frac{l_{v'}}{\|\boldsymbol{v}_g^0\|}\ \gamma(0). \tag{3.9}$$

In the Fourier space, the current Absolute Diffusivity Spectral Densisty (ADSD) (Resseguier et al, 2020) associated with the wave dynamics is defined by

$$A^{X_r}(k) = \frac{1/k}{\|\boldsymbol{v}_g^0(\boldsymbol{k}^{X_r})\|}\ E_k(k), \tag{3.10}$$

where $\boldsymbol{k}^{X_r}$ denotes the wave wave-vector, k the current wave number and E_k the current kinetic energy spectra. Accordingly, for noise calibration, we assume A^{X_r} self-similar and we choose a divergence-free spatial filter $\boldsymbol{\nabla}^\perp\psi_\sigma$ such that $\boldsymbol{v}' = \boldsymbol{\sigma}\mathrm{d}B_t/dt = \boldsymbol{\nabla}^\perp\breve{\psi}_\sigma \star \mathrm{d}B_t/dt$ and $\|\widehat{\boldsymbol{\sigma}\mathrm{d}B_t}(\boldsymbol{k})\|^2/dt = |k\ \widehat{\breve{\psi}_\sigma}(k)|^2 = A_{v'}^{X_r}(k)$.

3.3 A practical estimation

To simplify (3.3), let us consider the solution for an homogeneous and isotropic small-scale velocity $\boldsymbol{v}' = \boldsymbol{\sigma}\mathrm{d}B_t/dt = \boldsymbol{\nabla}^\perp\breve{\psi}_\sigma\star\mathrm{d}B_t/dt$ and Matérn stream function covariance, $(\breve{\psi}_\sigma * \breve{\psi}_\sigma)$, leading to

$$\boldsymbol{D} = \frac{1}{2dt}\begin{bmatrix} \mathbb{E}\left\{(\boldsymbol{\sigma}\mathrm{d}B_t)(\boldsymbol{\sigma}\mathrm{d}B_t)^T\right\} & \begin{matrix}0\ 0\\0\ 0\end{matrix} \\ \begin{matrix}0\ 0\\0\ 0\end{matrix} & \sum_{ij=1}^2 k_i k_j\ \mathbb{E}\left\{(\boldsymbol{\nabla}_{\boldsymbol{x}}(\boldsymbol{\sigma}\mathrm{d}B_t)_i)(\boldsymbol{\nabla}_{\boldsymbol{x}}(\boldsymbol{\sigma}\mathrm{d}B_t)_j)^T\right\}\end{bmatrix}, \tag{3.11}$$

$$= \begin{bmatrix} \frac{a_0}{2}\mathbb{I}_d & \begin{matrix}0\ 0\\0\ 0\end{matrix} \\ \begin{matrix}0\ 0\\0\ 0\end{matrix} & \frac{c_{\kappa_M}}{2}\left(\boldsymbol{k}\boldsymbol{k}^T + 3\boldsymbol{k}^\perp\left(\boldsymbol{k}^\perp\right)^T\right)\end{bmatrix}, \tag{3.12}$$

where $a_0 = \frac{1}{2dt}\mathbb{E}\|\boldsymbol{\sigma}\mathrm{d}B_t\|^2$ and $c_{\kappa_M} = \frac{1}{8dt}\mathbb{E}\|\nabla_{\boldsymbol{x}}(\boldsymbol{\sigma}\mathrm{d}B_t)^T\|^2$ are constants depending on both the correlation length and the spectrum slope of the small-scale velocity. The Ito action spectrum equation (3.2) then reads:

$$\begin{aligned}
&\partial_t N + \boldsymbol{v}_g \cdot \boldsymbol{\nabla}_{\boldsymbol{x}} N + \left(-\boldsymbol{\nabla}_{\boldsymbol{x}} \boldsymbol{v}^T \boldsymbol{k}\right) \cdot \boldsymbol{\nabla}_{\boldsymbol{k}} N \\
&= \boldsymbol{\nabla}_{\boldsymbol{x}} \cdot \left(\tfrac{1}{2} a_0 \boldsymbol{\nabla}_{\boldsymbol{x}} N\right) + \boldsymbol{\nabla}_{\boldsymbol{k}} \cdot \left(\tfrac{1}{2} c_{\kappa_M} \left[\boldsymbol{k}\boldsymbol{k}^T + 3\boldsymbol{k}^{\perp} \left(\boldsymbol{k}^{\perp}\right)^T \right] \boldsymbol{\nabla}_{\boldsymbol{k}} N \right), \qquad (3.13) \\
&= \tfrac{1}{2} a_0 \Delta_{\boldsymbol{x}} N + \tfrac{1}{2} c_{\kappa_M} \frac{1}{\|\boldsymbol{k}\|} \partial_{\|\boldsymbol{k}\|} \left(\|\boldsymbol{k}\|^3 \partial_{\|\boldsymbol{k}\|} N \right) + 3 \tfrac{1}{2} c_{\kappa_M} \partial^2_{\theta_k} N. \qquad (3.14)
\end{aligned}$$

The ensemble mean then follows :

$$\begin{aligned}
&\partial_t \mathbb{E}N + \overline{\boldsymbol{v}}_g \cdot \boldsymbol{\nabla}_{\boldsymbol{x}} \mathbb{E}N + \left(-\boldsymbol{\nabla}_{\boldsymbol{x}} \overline{\boldsymbol{v}}^T \boldsymbol{k}\right) \cdot \boldsymbol{\nabla}_{\boldsymbol{k}} \mathbb{E}N \\
&= \tfrac{1}{2} a_0 \Delta_{\boldsymbol{x}} \mathbb{E}N + \tfrac{1}{2} c_{\kappa_M} \frac{1}{\|\boldsymbol{k}\|} \partial_{\|\boldsymbol{k}\|} \left(\|\boldsymbol{k}\|^3 \partial_{\|\boldsymbol{k}\|} \mathbb{E}N \right) + 3 \tfrac{1}{2} c_{\kappa_M} \partial^2_{\theta_k} \mathbb{E}N, \qquad (3.15)
\end{aligned}$$

This last RHS diffusion term along the ray-direction θ is then reminiscent to Eq. 3.16 in Bôas and Young (2020) and Eq. 36 in Smit and Janssen (2019) derived under the same isotropic and homogeneous turbulence assumptions.

4 Numerical simulations

To illustrate our purpose, we consider the Surface Quasi-Geostrophic dynamics (Pierrehumbert, 1994; Lapeyre, 2017), abbreviated SQG:

$$\left(\partial_t + \boldsymbol{v} \cdot \boldsymbol{\nabla}\right) \left(-\frac{b}{N}\right) = 0 \quad \text{with} \quad \boldsymbol{v} = \boldsymbol{v}_{\mathrm{SQG}} = -\boldsymbol{\nabla}^{\perp}(-\Delta)^{-1/2} \left(-\frac{b}{N}\right). \quad (4.1)$$

Note, real-upper-ocean currents may not strictly follow SQG. Still, after a wind burst, it can be a good approximation at many mid-latitude locations. SQG corresponds to dynamics with extreme locality, i.e a KE spectrum with a shallow slope $-5/3$. Hence, for fixed KE value, a larger current gradient $\|\boldsymbol{\nabla}\boldsymbol{v}^T\|$ is expected. The validity of the time-decorrelation assumption of section 3 will then depend upon the scale separation, defining the correlation length of the unresolved scales.

A reference simulation is obtained at a resolution 512×512 for a 1000-km squared domain, through a pseudo-spectral code (Resseguier et al, 2017, 2020). Once initialized, the current velocity $\boldsymbol{v}$ is about 0.1 m.s^{-1}.

A swell system enters the southern boundary, propagating to the north. The carrier incident wave has a wave length $\lambda = 250$ m. Its envelope is Gaussian with an isotropic spatial extension of 30λ. Figure 1 illustrates the branched regime in this homogeneous SQG turbulence. This regime spreads the positions (left panel) and wavevectors (right panel) of the incoming waves. From south to north, spectral diffusion occurs (right panel), in the direction orthogonal (here k_x) to the propagation (here k_y). This accelerates – along the propagation – the zonal wave position spread, to create the branched regime visible in the left

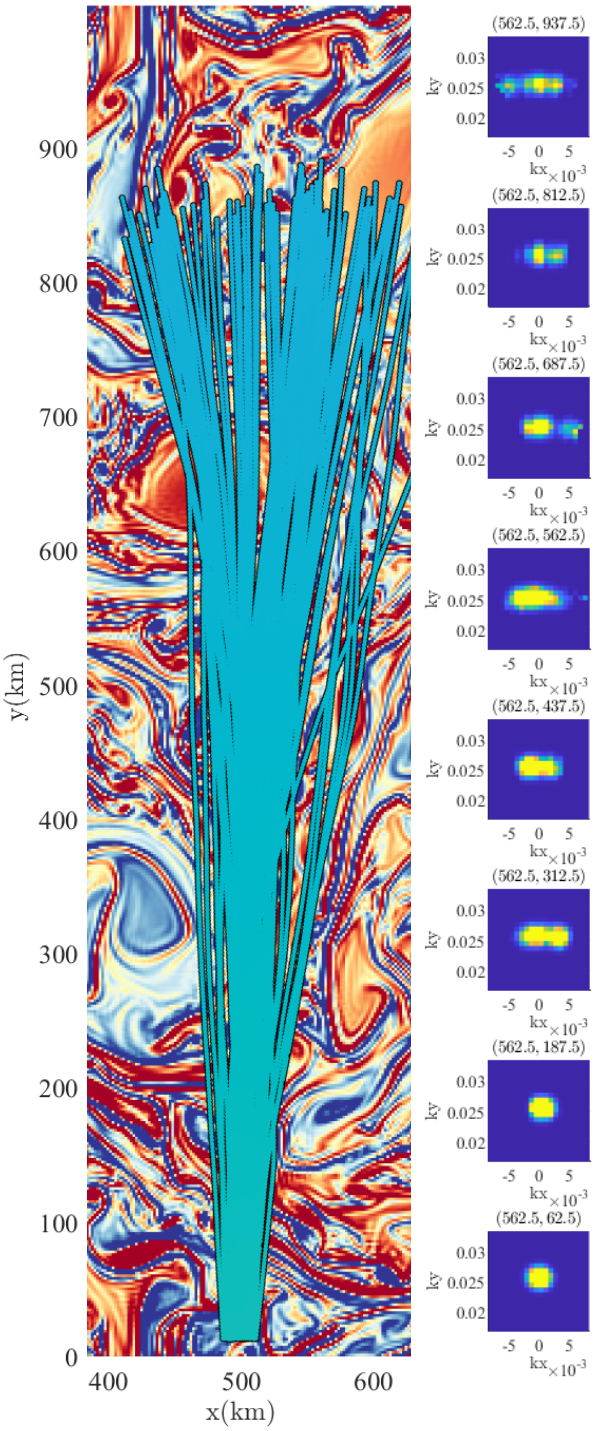

Fig. 1: Swell interacting with a high-resolution (512×512) deterministic SQG current. The left panel shows ray trajectories computed by forward advection and superimposed on the current vorticity $\omega = \boldsymbol{\nabla}^{\perp} \cdot \boldsymbol{v}$. The right panel shows bidirectional wave spectra, computed by backward advection, at 8 locations along a meridional axis (the mean wave propagation direction).

panel. This acceleration is explained by the ray equation (2.1) dominated by the intrinsic wave group velocity $\boldsymbol{\nabla}_{\boldsymbol{k}}\omega_0 = \frac{\|\boldsymbol{\nabla}_{\boldsymbol{k}}\omega_0\|}{\|\boldsymbol{k}\|}\boldsymbol{k}$.

To mimic a badly resolved $\overline{\boldsymbol{v}}$, the current $\boldsymbol{v}$ is smoothed at a resolution 32×32. Wave dynamics, using this coarse-scale current, are obtained Figure 2. The branched regime is strongly weakened, i.e. the spectral small-scale turbulence diffusion is missing.

A stochastic current is then added to this coarse deterministic one. That stochastic component is divergence-free and has a self-similar distribution of energy across spatial scales. Its precise parametrisation is a modification of the ADSD calibration (Resseguier et al, 2020) (see section 3.2). Figure 3 displays the wave simulations. This white-in-time model appears to work for a sufficiently well-resolved large-scale current. Indeed, the decorrelation ratio $\epsilon = (l_{v'}/\|\boldsymbol{v}_g^0\|)\|\boldsymbol{\nabla}\boldsymbol{v}^T\|$ depends on this resolution through $l_{v'}$. Specifically, for this SQG flow, the large-scale current $\overline{\boldsymbol{v}}$ needs to be resolved at least on a 32×32 grid, i.e. with a resolution $l_{v'} = 31.3$ km. As such, we obtain $\epsilon = 3.23 \times 10^{-2}$ (computed with $1/\|\boldsymbol{\nabla}\boldsymbol{v}^T\| = 1.38 \times 10^5$ s and $C_g \simeq 10$ m.s^{-1}).

5 Conclusion

The presence of velocity variations results in random scattering of swell-wave rays. Interactions are weak, but cumulative effects can become significant, to increase the average path length taken by the swell energy to reach an observer. Nowadays, sufficiently precise measurements can then open the possibility to use along-ray measurements to probe the near-surface ocean turbulence. Under a Lagrangian time-decorrelation assumption and using geometrical optics, a practical stochastic framework helps express these scattering effects on the mean swell-action statistics, directly in terms of the KE spectrum of the unresolved surface current field. Results are presented in both Lagrangian and Eulerian forms, where the latter augments the initial radiative transport equation with a diffusive term in directional space. Measured delays in swell arrivals, estimated wave height spectral characteristics and decays, and/or varying directional spread of the swell field shall then be more quantitatively interpreted to infer regional and seasonal upper ocean dynamical properties.

Acknowledgment

This work is supported by the R&T CNES R-S19/OT-0003-084, the ERC project 856408-STUOD, the European Space Agency World Ocean Current project (ESA Contract No. 4000130730/20/I-NB), and SCALIAN DS.

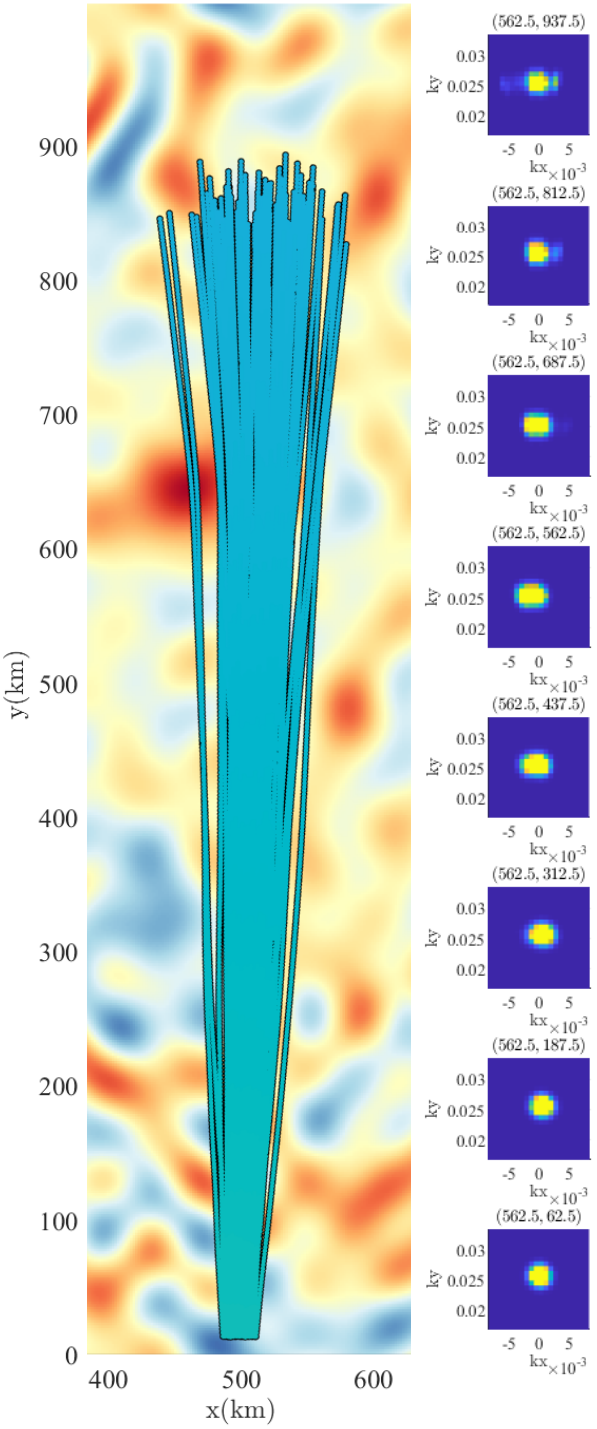

Fig. 2: Swell interacting with a low-resolution (32×32) deterministic SQG current. The left panel shows ray trajectories computed by forward advection and superimposed on the low-resolution current vorticity $\overline{\omega} = \boldsymbol{\nabla}^{\perp} \cdot \overline{\boldsymbol{v}}$. The right panel shows bidirectional wave spectra, computed by backward advection, at 8 locations along a meridional axis (the mean wave propagation direction).

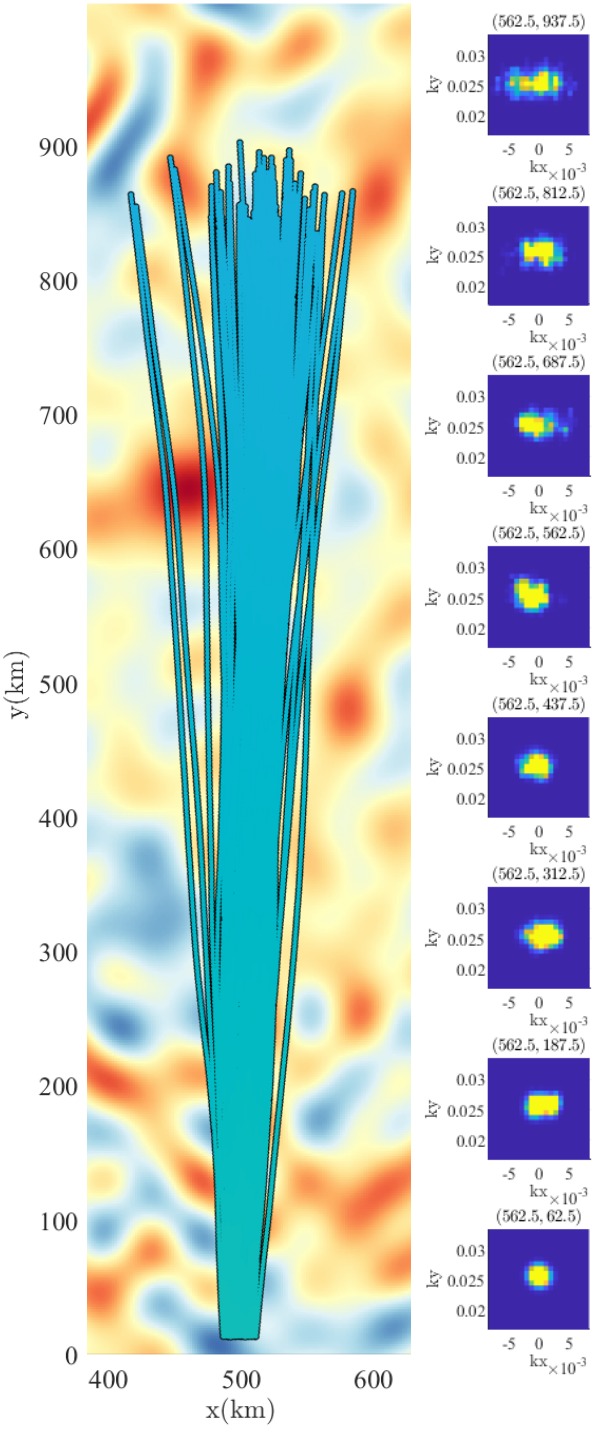

Fig. 3: Swell interacting with a low-resolution (32×32) deterministic SQG current plus (one realization of) the time-uncorrelated stochastic model. Ray trajectories are computed by forward advection and superimposed on the low-resolution current vorticity $\overline{\omega} = \boldsymbol{\nabla}^{\perp} \cdot \overline{\boldsymbol{v}}$.

Bibliography

Ardhuin F, Chapron B, Collard F (2009) Observation of swell dissipation across oceans. Geophysical Research Letters 36(6)

Ardhuin F, Gille ST, Menemenlis D, Rocha CB, Rascle N, Chapron B, Gula J, Molemaker J (2017) Small-scale open ocean currents have large effects on wind wave heights. Journal of Geophysical Research: Oceans 122(6):4500–4517

Bôas ABV, Young WR (2020) Directional diffusion of surface gravity wave action by ocean macroturbulence. Journal of Fluid Mechanics 890

Collard F, Ardhuin F, Chapron B (2009) Monitoring and analysis of ocean swell fields from space: New methods for routine observations. Journal of Geophysical Research: Oceans 114(C7)

Kunita H (1997) Stochastic flows and stochastic differential equations, vol 24. Cambridge university press

Lapeyre G (2017) Surface quasi-geostrophy. Fluids 2(1):7

Lavrenov I (2013) Wind-waves in oceans: dynamics and numerical simulations. Springer Science & Business Media

Oksendal B (1998) Stochastic differential equations. Spinger-Verlag

Phillips M (1977) The Dynamics of the Upper Ocean. Cambridge University Press

Pierrehumbert R (1994) Tracer microstructure in the large-eddy dominated regime. Chaos, Solitons & Fractals 4(6):1091–1110

Quilfen Y, Chapron B (2019) Ocean surface wave-current signatures from satellite altimeter measurements. Geophysical Research Letters 46(1):253–261

Resseguier V, Mémin E, Chapron B (2017) Geophysical flows under location uncertainty, part II quasi-geostrophy and efficient ensemble spreading. Geophysical & Astrophysical Fluid Dynamics 111(3):177–208

Resseguier V, Pan W, Fox-Kemper B (2020) Data-driven versus self-similar parameterizations for stochastic advection by lie transport and location uncertainty. Nonlinear Processes in Geophysics 27(2):209–234

Smit PB, Janssen TT (2019) Swell propagation through submesoscale turbulence. Journal of Physical Oceanography 49(10):2615–2630

Snodgrass FE, Groves GW, Hasselmann K, Miller GR, Munk WH, Powers WH (1966) Propagation of ocean swell across the pacific. Philos Trans R Soc London, Ser A (249):431â497

Voronovich A (1991) The effect of shortening of waves on random currents. In: Proceedings of nonlinear water waves, Bristol

White BS, Fornberg B (1998) On the chance of freak waves at sea. Journal of fluid mechanics 355:113–138